

*Modelling hydrological impacts of agricultural expansion in two macro-catchments in Southern Amazonia, Brazil*

Article

Accepted Version

Lamparter, Gabriele, Nobrega, Rodolfo, Kovacs, Kristof, Amorim, Ricardo Santos and Gerold, Gerhard (2018) Modelling hydrological impacts of agricultural expansion in two macro-catchments in Southern Amazonia, Brazil. *Regional Environmental Change*, 18 (1). pp. 91-103. ISSN 1436-3798 doi: <https://doi.org/10.1007/s10113-016-1015-2> Available at <https://centaur.reading.ac.uk/75081/>

It is advisable to refer to the publisher's version if you intend to cite from the work. See [Guidance on citing](#).

To link to this article DOI: <http://dx.doi.org/10.1007/s10113-016-1015-2>

Publisher: Springer Berlin Heidelberg

All outputs in CentAUR are protected by Intellectual Property Rights law, including copyright law. Copyright and IPR is retained by the creators or other copyright holders. Terms and conditions for use of this material are defined in the [End User Agreement](#).

[www.reading.ac.uk/centaur](http://www.reading.ac.uk/centaur)

**CentAUR**

Central Archive at the University of Reading

Reading's research outputs online

1 Modelling hydrological impacts of agricultural expansion in two macro-catchments in  
2 Southern Amazonia, Brazil

3  
4 Dr. Gabriele Lamparter<sup>1</sup>, [glampar@gwdg.de](mailto:glampar@gwdg.de)  
5 Rodolfo Luiz Bezerra Nobrega<sup>1</sup>, [rnobreg@gwdg.de](mailto:rnobreg@gwdg.de)  
6 Kristof Kovacs<sup>1</sup>, [kkovacs@gwdg.de](mailto:kkovacs@gwdg.de)  
7 Dr. Ricardo Santos Amorim<sup>2</sup>, [rsamorim@ufmt.br](mailto:rsamorim@ufmt.br)  
8 Prof. em. Gerhard Gerold<sup>1</sup>, [ggerold@gwdg.de](mailto:ggerold@gwdg.de)  
9

10 <sup>1</sup>Department of Physical Geography, University of Göttingen, Germany

11 <sup>2</sup>FAMEVZ (Faculdade de Agronomia e Medicina Veterinária), UFMT, Cuiabá, Brazil

12  
13 Gabriele Lamparter  
14 Institute of Geography,  
15 Department of Physical Geography  
16 University of Göttingen  
17 Goldschmidtstr.5  
18 37077 Göttingen  
19 0049-551-308026  
20 [glampar@gwdg.de](mailto:glampar@gwdg.de)

21 Abstract:

22 This study presents the setup, calibration, validation and scenario application of the Soil and Water  
23 Assessment Tool (SWAT) for two contrasting macro-catchments along the Amazon agricultural  
24 frontier in the federal states of Pará and Mato Grosso, Brazil. Calibration and validation of the model  
25 is realised for the periods of the most intensive deforestation and agricultural expansion. In order to  
26 give consideration to the rapid, however gradual nature of land use change, the model implements  
27 an annual land use update combined with a land use dependent soil parameterization of the upper  
28 most soil layer. The comparison of these results with the results of a setup with a steady land use  
29 distribution shows distinct improvements of the prediction quality. Discharge prediction improves  
30 through the application of gradual land use change in the model by 12% for a 1.8% deforestation rate  
31 per year and 1.2% for a deforestation rate of 0.7% per year. Consequently, the validated models are  
32 applied to four land use scenarios for the period 2026 to 2035. Scenario simulation results show  
33 effects on the water balance proportional to land use change. Further, the changes in the water  
34 balance follow clear seasonal patterns with highest hydrological effects due to land use change  
35 during the rainy season in both catchments. Overall, with continuous deforestation peak discharge  
36 increases. Further, the conversion of native to pasture has the highest impact on the water balance.  
37 For example, monthly discharge in the rainy season increases by up to 24% for a 13% conversion of  
38 Cerrado savannah into pasture.

39  
40 Keywords: hydrological catchment model, SWAT, water balance components, land use change, land  
41 use update, land use and climate scenarios, Amazon agricultural frontier

42 Length: Abstract: 252, Text body: 5628 words, References: 2589 words, TOTAL: 8609

43 Figures: 4, Tables: 3

44 1. Introduction:

45 The ever growing global demand for commodities rapidly pushes the agricultural frontiers around the  
46 world further into pristine nature and causes intensification on already existing farmland (Lambin *et al.*,  
47 2001). This is connected to changes in the hydrological balance. For example many studies find  
48 that deforestation leads to an increase in discharge (Q, D'Almeida *et al.*, 2007; Davidson *et al.*, 2012),  
49 higher floods and more severe water scarcity (Bruijnzeel, 2004; D'Almeida *et al.*, 2007; Fearnside,  
50 2007; Rodrigues *et al.*, 2009). Also other effects, such as changes in the seasonality and the reduction  
51 of storage capacity, are frequently reported (Bosch and Hewlett 1982). These changes are further  
52 alarming due to their potential to fuel problems connected to the effects of Climate Change (CC,  
53 Davidson *et al.*, 2012; Miles *et al.*, 2006). Still, responses to Land Use Change (LUC) are highly variable  
54 and depend on the spatial heterogeneity of land use and soil characteristics (Almeida *et al.* 2006 and  
55 2007). Therefore, it is not surprising that effects of current and future LUC on the hydrological  
56 balance, especially of macro-catchments, often remain poorly understood (Bruijnzeel, 2004; Coe *et al.*  
57 *et al.*, 2009; De Roo *et al.*, 2001; DeFries and Eshleman, 2004; Price, 2011).

58 The largest agricultural frontier with historic and current rapid LUC is located in Southern Amazonia  
59 in Brazil (Arima *et al.*, 2011; Fearnside, 2005, 2007). Figure 1 shows the natural vegetation of Brazil,  
60 the national highway BR-163 and the Amazon agricultural frontier. Due to its favorable climate for  
61 rainfed agriculture, Cerrado - the Brazilian savannah - is under extreme pressure from LUC (Beuchle  
62 *et al.*, 2015; Miles *et al.*, 2006). Historically, the deforestation of Cerrado vegetation was the most  
63 important source of new farmland in Brazil. Now, the Amazon agricultural frontier expands further  
64 towards the North through deforestation of rainforest (Arima *et al.*, 2011), a process boosted by the  
65 accessibility through new roads (Wertz-Kanounnikoff, 2005). The ongoing paving of the BR-163 in  
66 Central Brazil lead to these typical frontier colonisation processes since the 1990s (Fearnside, 2005).

67 Only a few macro-catchment studies in the Cerrado biome evaluate the hydrological effects of this  
68 comprehensive LUC. However, these studies consistently show a rising trend in Q with deforestation.  
69 For example, Costa *et al.* (2003) showed an increase of Q for the Tocantins River (of which the das  
70 Mortes River is a tributary) and an analysis of decadal runoff by Guzha *et al.* (2013b) showed a rise in  
71 runoff between 1968 and 1987 for the das Mortes River at Toriquejé (which coincides with 40%  
72 Cerrado removal). Macro-catchment LUC research in the rainforest biome is more common.  
73 However, these studies show contradictory results regarding hydrological effects (Coe *et al.*, 2009;  
74 Lima *et al.*, 2013).

75 Hydrological models aid the understanding and enable the prediction of changes in the water  
76 balance components (WBC) due to future development. However, a reliable prediction of  
77 hydrological responses depends on an accurate formal model description of the relevant processes  
78 (Beven, 2010), e.g. processes connected to LUC. Typically, the long-term effects of LUC on hydrology  
79 are investigated with models calibrated with a steady land use distribution, which is subsequently  
80 applied to scenarios with a different and again steady land use distribution (Coe *et al.*, 2009). Here,  
81 parameters connected to the different vegetation or land use types of the calibration and scenario  
82 periods are determined prior to the model application. This means that hydrological effects of LUC  
83 are present in these parameters. Hence, the effects of LUC in a scenario application is predetermined  
84 and not tested with observed effects of LUC on hydrology. In this study, we allow the model to adapt  
85 land use related parameters to observed hydrological LUC effects by including the gradual nature of  
86 LUC in the calibration procedure. The SWAT model is an eco-hydrological model (here version  
87 SWAT2012, for documentation see Arnold *et al.*, 2012; Gassman *et al.*, 2007) which includes the  
88 possibility of gradual temporal changes on a daily basis (Pai and Saraswat, 2011). Only a few studies

89 have implemented gradual land use change in their SWAT models (Chiang *et al.*, 2010; George, 2014;  
90 Guse *et al.*, 2015; Koch *et al.*, 2012; Mani *et al.*, 2014; Wagner *et al.*, 2016). Even fewer have included  
91 an evaluation of the performance of the included gradual LUC in the calibration and validation period  
92 (Guse *et al.*, 2015; Koch *et al.*, 2012).

93 Aims and objective:

94 Therefore, we present here a study simulating the hydrological effects during the rapid historic LUC  
95 in the calibration and validation period for two contrasting macro-catchments: the das Mortes  
96 catchment with 17,556 km<sup>2</sup> in the Cerrado biome (-15.14°, -54.16°) and the Jamanxim catchment with  
97 37,403 km<sup>2</sup> in the Amazon rainforest biome (-7.34°, -55.84°) including the gradual nature of LUC into  
98 the model setup. Furthermore, we assess in how far the inclusion of gradual LUC improves the model  
99 prediction by comparing the gradual LUC model setup to a setup with steady land use distribution.  
100 Lastly, the calibrated model for both catchments is put into practice for scenarios of future LUC with  
101 identical climate scenarios for the period 2026 to 2035 to estimate the magnitude of hydrological  
102 changes dependent on potential future LUC.

103 2. Study area and period:

104 The two catchments were chosen in areas of rapid historic deforestation and dominant rainfed  
105 agriculture to ensure that LUC effects are not influenced by technical water management (e.g. dams  
106 and irrigation). The das Mortes catchment is situated in the federal state of Mato Grosso. It is located  
107 on top of a plateau of cretaceous sandstone maintaining a large deep aquifer (Schneider, 1963). The  
108 climate is tropical wet and dry (dry period: May to September, Climate-Data.org, 2015), with an  
109 precipitation (P) of 1784 mm a<sup>-1</sup> (Primavera do Leste, Global Weather Data, 2015). The dominant soil  
110 types are the highly permeable Ferralsol (70%) and Arenosol (23%, see the Brazilian Agricultural  
111 Research Corporation (EMPRAPA) soil map profiles, ESALQ, 2015). The average slope is 2.9%. Mato  
112 Grosso is the Brazilian state with the highest deforestation rate (Macedo *et al.*, 2012). Deforestation  
113 rates are declining since 2000 (Davidson *et al.* 2012) due to exhaustion of forested areas on arable  
114 soils which are not protected in reservations. Parallel to the slowing deforestation in the last 15-20  
115 years, land use in Mato Grosso and especially in the das Mortes catchment is characterised by  
116 intensification with a shift towards double cropping and minimum tillage (Beuchle *et al.*, 2015;  
117 Galford *et al.*, 2010; Hunke *et al.*, 2015b). For the das Mortes catchment, the historic land use  
118 classification was realised with Landsat satellite imagery analysis by Schlicht (2013) with an accuracy  
119 of 97% and an omission error of less than 1% (for 1988 and 1998). Deforestation for 1970 prior to be  
120 the first Landsat image was 1% (IBGE, 2015). Consequently, the mid-1970s to mid-1980s are  
121 identified as the period with the most intensive deforestation in this area (Table 1). This coincides  
122 with the period 1968-1987 for which Guzha *et al.* (2013b) showed an increase in Q despite steady P  
123 records. For the das Mortes catchment, satellite and statistical information is not sufficient to reliably  
124 distinguish between cropland and pasture land uses. Consequently, the land use category "Non-  
125 Forest" was defined.

126 The Jamanxim catchment is located in the central southern part of the Amazon rainforest in the state  
127 of Pará. Its geological structure consists of Ordovician sedimentary and Precambrian metamorphic  
128 rocks (usouthal.edu, 2016). It has a tropical monsoon climate and a dry period from June to August  
129 (Climate-Data.org, 2015) with an annual P of 2232 mm (Novo Progresso, Global Weather Data, 2015).  
130 The dominant soil type is the deeply weathered Acrisol (84%, see ZEE, 2015). The average slope is  
131 12.7%. The historic land use classification was realised with Landsat satellite imagery by Macioscheck  
132 (2013, for 1998, 2007 and 2011) with an accuracy of 99% (Maciocheck, 2013). Deforestation rates  
133 peaked in the 2000s to open up pastures for cattle grazing. Compared to the total Brazilian Amazon

134 Basin, pre 1990 deforestation in the Jamanxim catchment was comparatively low, increasing rapidly  
135 in the 1990s and 2000s, now reaching 15% (see Tabel 1).

136 For the das Mortes catchment, the period from 1977 to 1981 was chosen for calibration and 1982 to  
137 1986 for validation. This period combines good Q and P records, the most rapid LUC and a change in  
138 the relationship of Q and P. In the Jamanxim catchment the most rapid deforestation occurred in the  
139 last decade. Further, a longer time series of Q is only available from 2000 to 2009. Consequently, this  
140 period was chosen, with 2000 to 2004 for calibration and 2005 to 2009 for validation.

141 Furthermore, the scenario application in both catchments was set to the decade around the year  
142 2030. Future LUC in the region is mainly dependent on political, economic and social development.  
143 The LANDSHIFT model (Schaldach *et al.*, 2011; Schaldach and Koch, 2009) has the capability to  
144 estimate future LUC along storylines sketching political, economic and social development. For the  
145 two study regions, four different scenarios developed in an interdisciplinary effort by the Carbiocial  
146 project (carbiocial.de, Schöenberg *et al.*, this issue) are taken into account: A *trend* scenario, where  
147 the development seen in the last decade will continue into the future, a *sustainable* scenario where  
148 regulations favour sectors with the most efficient land use, i.e. reduction of cattle ranching and a  
149 focus on crop production. Further, both the *legal* and *illegal* scenarios suggest a rapid agriculture  
150 expansion, either *legal* with the perpetuation of current protective areas or *illegal* without (for a  
151 detailed description refer to Göpel and Schaldach, this issue). The fractions of the land use in 2020,  
152 2025 and 2030 of the four LANDSHIFT calculated scenarios are also listed in Table 1. The land use  
153 distribution in the das Mortes catchment does not ideally reflect the overall development associated  
154 with the scenarios. For example, the *illegal* scenario displays the highest fraction of scrubland  
155 vegetation (Cerrado). The *trend* scenario is marked with a 12-14% higher fraction of pasture. The  
156 highest fraction of cropland is associated with the *sustainable* scenario and continuously declines  
157 from *legal* to *illegal* to *trend* scenario. For the Jamanxim catchment, the scenario differences are as  
158 intended with the highest remaining forest cover and a complete elimination of pasture for the  
159 *sustainable* scenario. In 2030, the *legal* and *illegal* scenarios show a land use with 23% more forest  
160 clearance in 2030 compared to the *sustainable* scenario. However, they display different  
161 deforestation rates in the years before where the *legal* scenario behaves similar to the *sustainable*.  
162 Furthermore, deforestation is distributed differently over the catchment. The *trend* scenario has an  
163 intermediate fraction of forest removal and an intermediate extend of pasture.

164

### 165 3. Setup and parametrisation of the SWAT2012 model

#### 166 a. Topography:

167 The SWAT model depends on a distributed representation of the catchment geometry and its river  
168 network (here, ASTER data sets (version 2) with 30 m grid cell resolution). It was delineated for the  
169 catchment outlet points at Toriquejé in the das Mortes catchment (-15.25°, -53.06°) and at Jardim do  
170 Ouro in the Jamanxim catchment (-5.50°, -55.83°). For the das Mortes catchment, sub-catchments  
171 are as best determined according to municipality borders to utilise information from the Brazilian  
172 Institute of Geography and Statistics (IBGE). In the Jamanxim catchment, sub-catchments include  
173 areas with similar land use.

#### 174 b. Hydrological Response Unit (HRU) definition and management operations:

175 For each sub-catchment HRUs with a unique soil, slope and land use are defined. SWAT allows the  
176 selective parametrisation of these smallest units of execution. The management in the das Mortes  
177 catchment includes double cropping (soy and corn) and cattle grazing for Non-Forest, depending on  
178 the soil type (good quality leads to cropping, poor quality to grazing). No management is

179 implemented in Cerrado and gallery forest HRUs. For the Jamanxim catchment only HRUs with  
180 pasture are managed with cattle grazing.

181 c. Vegetation parametrisation

182 Parametrisation of new land use types were added to the SWAT2012 data base using a combination  
183 of literature data and own observations. Parameters for Cerrado and gallery forest were extracted  
184 from a range of eco-physiological and hydrological studies (Coe *et al.*, 2009; Davidson *et al.*, 2012;  
185 Lathuillière *et al.*, 2012; Pongratz *et al.*, 2006). For pasture, the SWAT 2012 database was extended  
186 with area specific information (Allen *et al.*, 1998; Barona *et al.*, 2010; Hayhoe *et al.*, 2011; Lathuillière  
187 *et al.*, 2012). Also, rainforest was added using literature information (Granier *et al.*, 2000; Hayhoe *et al.*  
188 *et al.*, 2011; Kergoat, 1998; Sellers *et al.*, 1989, 1996). A particular challenge is SWAT's dependency on  
189 the dormancy during the winter season for the reinitiation of the growing season for perennial  
190 plants. This process is not a valid growing pattern in the tropics. Therefore, the plant growth  
191 modification of Strauch and Volk (2013) - originally developed for the Cerrado biome - was applied  
192 for Cerrado, rainforest, gallery forest and pasture. Here, the start of the growing season is triggered  
193 by an increase of available soil water. Evapotranspiration and leaf area index (LAI) curves were  
194 adjusted by manually changing SWAT specific parameters determining the LAI curve shape to match  
195 observations (Christoffersen *et al.*, 2014; Giambelluca *et al.*, 2009; Lima *et al.*, 1990; Oliveira, 2014;  
196 Oliveira *et al.*, 2014; Strauch and Volk, 2013).

197 d. Soil parametrisation

198 With regard to soil surface parametrisation, surface runoff (Q<sub>sur</sub>) and infiltration are determined by  
199 the SCS Curve Number (CN) method (Mishra and Singh, 2003). The initial parameter estimates are  
200 taken from Drewry *et al.* (2008); Hunke *et al.* (2015b); McGrath *et al.* (2001) and Oliveira *et al.*  
201 (2014). Mean values for soil texture and bulk density were determined through statistical analysis of  
202 the RADAM soil profile data base (ESALQ, 2015; Jacomine, 2013). Lastly, hydraulic conductivity ( $k_{sat}$ )  
203 for the main soil types was defined according to our own in situ measurements with a Compact  
204 Constant Head Permeameter (Amoozegar and Warrick, 1986).

205 e. Implementation of gradual land use change

206 The LUC for the calibration, validation and each scenario application was calculated separately in  
207 each sub-catchment and updated on an annual basis. The land use distribution for years without  
208 information was estimated with linear interpolation, also for each sub-catchment separately. On  
209 average during the calibration and validation periods, every year 1.8% of Cerrado vegetation was  
210 converted into Non-Forest in the das Mortes catchment. In the Jamanxim catchment, 0.7% forest  
211 was transformed into pasture. The LUC is concentrated in the Western parts of the catchment, which  
212 is crossed by the BR 163. The sub-catchments crossed by the BR 163 have a deforestation rate of  
213 2.4% p.a.. However, gradual LUC is connected to some shortcomings, since the SWAT land use  
214 update function allows only to redefine the fractions of existing HRUs, not the inclusion of new HRUs.  
215 In some cases it was not possible to redefine the land use class without also redefining either slope  
216 or soil class. In these cases areas of HRUs under LUC were preferable assigned to HRUs with the most  
217 similar soil type and slope class. Typically, for calibration, validation and scenario application this  
218 affected areas of less than 2.5%. Only in the case of the calibration and validation period in the Rio  
219 das Mortes 6% of the catchment area had to be reassigned from the Latosolo Vermelho-Amarelo to  
220 the Latosolo Vermelho soil class. Since this are small areas and in the case of the soil reassignment  
221 similar soil types, we do not expect this to causes considerable changes to water balance calculation.

222 f. Weather data:

223 The daily weather records from INMET and ANA (Instituto Nacional de Meteorologia, BDMEP 2015  
 224 and Agencia Nacional de Aguas, ANA 2015) are applied in the das Mortes catchment. The P records  
 225 are cross referenced for validity with CFSR reanalysed forecast data on a 35 km raster resolution  
 226 (Fuka *et al.*, 2014; Global Weather Data, 2015). For the das Mortes catchment, INMET and CFSR  
 227 weather data are on average similar. In the Jamaxim catchment, due to the lack of weather data  
 228 records, CFSR data is used as the source of weather information. Comparing the rainfall data with the  
 229 closest weather station in Itaituba shows that the CFSR data is overestimating P in the wet season  
 230 and underestimating P in the dry season. The Itaituba INMET station records an annual average of  
 231 2070 mm (1530 mm in the rainy season and 540 mm in the dry season) for the period from 1961 to  
 232 2010, whereas the mean of the CFSR data sets annual P to 2400 mm per annum (2105 mm in the  
 233 rainy season and 295 mm in the dry season) for 1979 to 2014. From this a P correction factor was  
 234 calculated for each month of the year which adapts the CFSR data to the level measured at Itaituba.  
 235 For all LUC scenarios, the IPPC SRES A1B climate scenario downscaled with the STAR method (Böhner  
 236 *et al.*, 2013; Böhner, this issue) for the period 2026 to 2035 is applied. The scenario predicts a  
 237 considerable reduction in annual P of 29% in the das Mortes catchment and 32% in the Jamaxim  
 238 catchment in comparison to the calibration and validation period.

239 g. Model calibration and validation:

240 The model calibration is based on the optimisation of the modelled monthly Q (Qmod) at the outlets  
 241 of the catchments towards the observed values (Qobs). The daily Q information (“ANA” 2015, station  
 242 2650000) was transferred into monthly values. Both the calibration, and the estimation of the  
 243 predictive uncertainty was automated with the software tool SWAT-CUP (Abbaspour, 2007) with the  
 244 Sequential Uncertainty Fitting (SUFI-2) method (Abbaspour *et al.*, 2004).

245 The calibration concentrates on two groups of calibration parameters: Firstly, parameters, which are  
 246 generally sensitive, such as groundwater related parameters. These are adapted in the calibration  
 247 procedure for the whole catchment. Secondly, parameters connected to land use, which are  
 248 parameters defining vegetation growth and properties of the upper soil, such as CN and  $k_{sat}$ . In the  
 249 calibration procedure these were adapted for each soil and land use type combination separately.  
 250 For all calibration parameters, physically meaningful ranges are defined as the parameter space.  
 251 From these, random samples are taken with the latin hypercube method (Abbaspour, 2007) for each  
 252 of the 1500 iterations for one calibration run.

253 At the end of the calibration run, the best estimation is identified with the Nash-Sutcliffe Efficiency  
 254 index (NS) as the objective function. Further, the coefficient of determination ( $R^2$ ), percentual bias  
 255 (PBIAS) and Root Mean Error (RME) are also calculated for the identified best estimation.

256 The uncertainty is calculated from the cumulative distribution of the output variable(s) ( $i_t$ ) for every  
 257 output time step ( $t$ , here monthly). The 95% confidence interval (95CI) is the range between the  
 258 2.5% and 97.5% levels of the distribution of  $i_t$ , which relates to the reliability of the estimation  
 259 procedure, not the probability of a value being estimated. Further, the p-factor (fractions of values  
 260 within 95CI) and the r-factor (relative bandwidth of 95CI =  $\frac{95CI_{max}-95CI_{min}}{(i_t mean+i_t sd)-(i_t mean-i_t sd)}$ ) are evaluated.

261 Each calibration run with 1500 iterations suggests a progressively smaller calibration parameter  
 262 range until the 95CI of the model output is close to the standard deviation of the measured data. In  
 263 order to generate comparable conditions for the calibration of the setup with and without gradual  
 264 land use change, the initially identical parameter space was set to half its range in each consecutive  
 265 calibration run. For each setup, calibration runs with 1500 iterations are repeated three times to  
 266 achieve the before mentioned quality criterion. The final calibration parameter range from the setup  
 267 with gradual land use change is then brought forward to be executed for the validation period (and  
 268 the steady land use model setup from 1988 for the das Mortes catchment and from 2007 for the



269 Jamanxim catchment). For the scenario application, only the optimum value for each calibration  
270 parameter defined through the setup including gradual land use change is implemented. In order to  
271 highlight the performance of the land use update setup, the predictive error ( $PE=Q_{obs}-Q_{mod}$ ) of the  
272 catchment discharge is evaluated. Further, the LOcally WEighted Scatterplot Smoothing (LOWESS) as a  
273 nonparametric regression using multiple regression models (Cleveland, 1981) is applied to PE to  
274 visualise trends concealed by the variability of PE.

#### 275 4. Results

##### 276 a. Optimum values of selected calibration parameters:

277 A calibration parameter with fundamental influence especially on the distribution of water between  
278 the rainy and the dry season is the groundwater delay factor (given in days). This is a calibration  
279 parameter independent of land use, which determines the baseflow ( $Q_{gw}$ ) contribution to discharge.  
280 Since very little is known about the groundwater dynamics in both catchments, this parameter was  
281 defined during the calibration procedure. It displays a clear difference between the two study  
282 catchments. In the das Mortes catchment,  $Q_{gw}$  makes up for ~80% of  $Q$ , fed by an extensive  
283 groundwater buffer, represented by an optimum groundwater delay of 316 days, maintaining  
284 minimum  $Q$  at 25% of the maximum  $Q$ . In the Jamanxim catchment,  $Q$  generation is foremost  
285 influenced by interflow ( $Q_{int}$ ), causing  $Q$  to be maintained at 5 to 10% of the maximum, which is  
286 associated with a much shorter groundwater delay of 74 days. This difference can be explained by  
287 the following characteristics of the catchments. The das Mortes catchment is dominated by a mostly  
288 flat relief (Guzha *et al.*, 2013a) with sandy soils, causing water to percolate freely to the deep aquifer.  
289 Further, it is underlain by a pan like geological structure of cretaceous sandstone supporting an  
290 aquifer of up to 1300 m depth (Parana Mesozoic and Paleozoic groundwater province, Schneider,  
291 1963). The Jamanxim catchment belongs to a greater part to the Central Precambrian groundwater  
292 province, which typically only supports a thin deep aquifer and wells with low yields (Schneider,  
293 1963). Further, the relief is comparable steep supporting a faster lateral runoff.  
294 There is strong evidence that LUC alters particularly the properties of the upper soil layer (Bruijnzeel,  
295 2004; Christoffersen *et al.*, 2014). Therefore, CN and  $k_{sat}$  of the upper most soil layer, which were  
296 initially parameterized according to soil type only, were adapted during the calibration procedure  
297 independent for each soil and land use type. Table 2 lists their land use dependent optimum values  
298 as suggested by the final iteration of the calibration runs with gradual land use change. Overall CN  
299 values are low, confirming the initial high infiltration into the upper soil layer in both catchments due  
300 to permeable soils. Nevertheless, the calibration procedure identified lower CN for natural  
301 vegetation compared to cropland and pasture. The calibration also suggests higher  $k_{sat}$  values for  
302 natural vegetation compared to pasture and cropland in both catchments. Such a change of  
303 properties in the upper soil layer with LUC is in accordance with own measurements and literature  
304 data (Christoffersen *et al.*, 2014; Hunke *et al.*, 2015a).

##### 305 b. Prediction quality:

306 The identified optimum calibration parameters result in a  $Q_{mod}$  in good accordance with  $Q_{obs}$ .  
307 Table 3 shows that if we are looking at NS both the das Mortes and the Jamanxim catchment have a  
308 very good to good performance rating for the calibration, validation of both land use update and  
309 steady land use application (Moriasi *et al.*, 2007). The values are well within the results reported for  
310 other macro-catchment models (Fukunaga *et al.*, 2015; Guzha *et al.*, 2013a; Nandakumar and Mein,  
311 1997; Schilling *et al.*, 2008). Divergences between the land use update and steady land use  
312 application for the das Mortes catchment are reflected in NS and the r-factor. NS is considerable  
313 higher for the calibration with gradual land use. Further, the r-factors of both the calibration and  
314 validation period in the das Mortes catchment are smaller than in the steady land use application.

315 Similar differences in the Jamanxim catchment are less pronounced, however perceivable. Here, the  
316 small fraction of areas with LUC (see Table 1) compared to the large area of remaining rainforest  
317 buffers the responses of the hydrological balance.

318 To highlight the different performance of the land use update and the steady land use setup, Figure  
319 2a shows the PE between  $Q_{obs}$  and model  $Q_{mod}$  for land use update ( $PE_1$ ) and steady land use ( $PE_2$ )  
320 setup in the das Mortes catchment. PE shows that both overprediction (negative PE) and  
321 underprediction (positive PE) are more pronounced for a steady land use setup ( $PE_2$ ). LOWESS  
322 regressions are applied to show the trend in PE over the application period. Both PEs decline towards  
323 the end of the period. Additionally, the difference between  $PE_1$  and  $PE_2$  declines, showing that the  
324 steady land use setup prediction becomes more accurate towards the date of the applied land use  
325 distribution (from the year 1988). Similar, but less pronounced differences can be seen in the PEs for  
326 the Jamanxim catchment in Figure 2b. Again, the steady land use setup has both a higher over- and  
327 underprediction of the observed discharge. If looking at the LOWESS regression, in the first seven  
328 years of the application period, the land use update setup shows a slightly lower underprediction  
329 compared to the steady setup. For the year 2007, the land use update  $PE_1$  and the steady land use  
330  $PE_2$  are the same.

### 331 c. Scenario application

332 The four LUC scenario applications in each catchment (for degree of LUC refer to Table 1) were  
333 executed with identical climate projections to reflect purely on alteration of WBCs due to LUC. Mean  
334 annual WBCs in relation to mean annual P for the scenario period from 2026 to 2035 are shown in  
335 Figure 3a and b. In the das Mortes catchment, the WBC in the *sustainable*, *legal* and *illegal* scenarios  
336 are of the same magnitude reflecting the distribution of land cover with only a gradual change of  
337 Cerrado and cropland. Only the *trend* scenario with the highest fraction of pasture results in a higher  
338 Q due to a lower evapotranspiration and  $k_{sat}$  reduction. Moreover, it is the scenario with the highest  
339 surface runoff, however rates are generally limited to less than  $1 \text{ mm month}^{-1}$ . Considerable surface  
340 runoff ( $> 10 \text{ mm month}^{-1}$ ) only occurs in the Western parts of the catchment (on Latosolo) during the  
341 very wet month of February in 2034 with more than 400 mm P causing soil saturation and therefore  
342 soil saturation excess runoff.

343 The land cover scenarios in the Jamanxim catchment show gradual differences between all scenarios.  
344 Differences in Q are mirrored in ET with the lowest Q and highest ET for the *sustainable* scenario with  
345 forest protection and an elimination of pastures. Surface runoff is limited to the steep headwater  
346 catchments in the south.

347 Additionally to the changes in the overall WBC, the seasonality of runoff generation changes. Figure 4  
348 shows monthly  $\Delta Q$  for the *sustainable*, *legal* and *illegal* scenario, where  $\Delta Q$  is the difference between  
349 Q of the *trend* scenario and Q of each of the other scenarios ( $\Delta Q = Q_{trend \text{ scenario}} - Q_{other \text{ scenarios}}$ ). For the  
350 seasonal comparison, the *trend* scenario Q is also plotted. The differences in mean Q are not  
351 distributed equally throughout the year but predominantly associated with the peak discharge  
352 months. In the das Mortes catchment, highest  $\Delta Q$  is found during rising Q at the beginning of the  
353 rainy season. Additionally, during the low flow period in dry years, the *trend scenario* maintains  
354 higher flows. The *trend* scenario has the highest proportion of pasture, which means that pasture  
355 generates more runoff at the beginning of the rainy season and higher  $Q_{gw}$  compared to the other  
356 land use types. This is in accordance with research showing that pasture causes higher peak  
357 discharge (Costa *et al.*, 2003; Drewry *et al.*, 2008; Guzha *et al.*, 2013b; Hodnett *et al.*, 1995; Hunke  
358 *et al.*, 2015a). We account this to the ready available leaf area resulting in immediate  
359 evapotranspiration (Cerrado) of the received P and a higher water storage capacity of the less  
360 compacted soil.

361 In the Jamanxim catchment, largest  $\Delta Q$ s are associated with the *sustainable* scenarios, with the  
362 highest fraction of remaining forest cover. The *trend* scenario has a land cover distribution similar to  
363 the *legal* and *illegal* scenario and therefore  $\Delta Q$ s are very low. The pattern of  $\Delta Q$  for the *sustainable*  
364 scenario follows a pattern of lower discharge, especially during the rising stage of the wet season and  
365 the maintenance of higher flows during the dry season.

366 This seasonal pattern is potentially characteristic for hydrological effects of LUC in areas with  
367 pronounced wet and dry periods, since it was also observed in a similar SWAT model application  
368 including gradual LUC by Wagner *et al.* (2016) for a catchment in India with monsoon climate.

## 369 5. Discussion:

370 For our catchments with intensive LUC in the calibration and validation period, the model setups  
371 including gradual land use change show a better performance than the model setups with a steady  
372 land use distribution. This is reflected in the throughout smaller PE of the land use update setup in  
373 the two contrasting catchments. The difference between the error calculations of the two setups is  
374 dependent on the degree of LUC. In the das Mortes catchment with 1.8% deforestation per annum,  
375 absolute PE<sub>1</sub> is on average 19 mm per annum smaller (corresponding to 11.2% Q or 1.8% P) than  
376 absolute PE<sub>2</sub>. For the Jamanxim catchment with 0.7% deforestation per annum, the difference is 8  
377 mm per annum (corresponding to 1.2% Q or 0.4% P).

378 Classically, land use influence on water balance is dependent on differences in evapotranspiration.  
379 Here we also included the differentiation of properties of the upper soil layer under different land  
380 use. For each land use and soil type combination, these are adapted independently in the calibration  
381 procedure. The calibration results support that LUC is accompanied by soil compaction processes  
382 through deforestation and agricultural land use. Remarkably, our results fit well with reported field  
383 research findings, regarding the soil compaction through land use in this area (Bruijnzeel, 2004;  
384 Christoffersen *et al.*, 2014; Drewry *et al.*, 2008; Hunke *et al.*, 2015b; Nobrega *et al.*, 2015; Scheffler *et al.*,  
385 2011). These established higher optimum CN and lower optimum  $k_{sat}$  values for cropland and  
386 pasture compared to natural vegetation have a clear effect on Q prediction. This agreement of field  
387 records and calibration outputs indicates an adequate representation of pedo-hydrological processes  
388 connected to LUC.

389 The model applications are an advanced tool to contribute to the discussion about changes of WBC  
390 due to future LUC, since they include both, the change of evapotranspiration and soil properties with  
391 LUC. Moreover, in many cases LUC effects on hydrology are subordinate to CC effect. Therefore, the  
392 different LUC scenarios are simulated with the same climate scenario to ensure that all observed  
393 hydrological effects are purely LUC effects. According to our results, for both the das Mortes and the  
394 Jamanxim catchment, the model shows an increase of Q with continuous deforestation. For the das  
395 Mortes catchment, a reduction of Cerrado of 5% and an increase of pasture of 12% (compare *illegal*  
396 to *trend* scenario 2030) results in an 3.4% increase of annual Q, which confirms findings of (Costa *et al.*,  
397 2003; Guzha *et al.*, 2013a). In the Jamanxim catchment, 24% more deforestation (compare  
398 *sustainable* to *illegal* scenario 2030) increases Q by 13 mm per annum (2.0% of Q, 0.8% of the P).  
399 However, Coe *et al.* (2009) and Lima *et al.* (2013) stress the fact, that P is dependent on recycled  
400 transpiration from the forest vegetation (P-feedback). This process is most effective in the rainforest  
401 biome, where studies state that with complete deforestation, P is reduced by 20 to 35% (D'Almeida  
402 *et al.*, 2007; De Paiva *et al.*, 2013; Nobre *et al.*, 1991). Coe *et al.* (2009) and Lima *et al.* (2013) both  
403 showed with the application of a model with and without P-feedback, that the inclusion of P-  
404 feedback is crucial for Q prediction in the Amazon rainforest biome. Our Jamanxim results are similar  
405 to the results of the Coe *et al.*, (2009) model without P-feedback, where a deforestation of 26% leads

406 to an 8% increase of Q, however, with P-feedback for the same area Coe *et al.* (2009) find Q to  
407 decrease by 12%. Consequently, for our model a more accurate prediction needs to include P-  
408 feedback. This cannot be realised in SWAT directly, but needs to be incooperated in the climate  
409 model. In the current STAR climate prediction an adaption of P according to the different LUC  
410 scenarios is not implemented, not least because of the complex nature of P-feedback, which is highly  
411 dependent on deforestation pattern (Negri *et al.*, 2004). However, our future research aims to  
412 include these complex feedbacks.

413 Independent of P-feedback effects, a comparison of scenarios suggests a severe influence of  
414 conversion into pasture on the WBC. In the das Mortes catchment, a 13% increase of pasture  
415 (compare *trend* and *sustainable* scenario) causes a 4 to 27 mm (13.3-73.0%) increase in monthly Q at  
416 the beginning of the rainy season (December and January) due to decreased evapotranspiration and  
417 an increase in Q<sub>sur</sub> and interflow (Q<sub>int</sub>, Fig. 4a). The differences in Q seasonality for increased Q due  
418 to pasture and cropland area are similar in the Jamanxim catchment. For example, 14% more  
419 cropland (compare *trend* and *legal* scenario in 2030) leads to up to 30 mm month<sup>-1</sup> higher discharge  
420 during the rainy season.

421

422 Conclusions:

- 423 • Through the implementation of gradual land use change, the accordance of Q<sub>mod</sub> and  
424 Q<sub>obs</sub> is improved by 11.2% in the catchment with 1.8% annual deforestation and by 1.2%  
425 in the catchment with 0.7% annual deforestation. This demonstrates that in regions with  
426 intensive LUC during the application of a hydrological model, the inclusion of gradual  
427 land use change is necessary to ensure the best possible prediction quality.
- 428 • The model predictions for four land use scenarios in two fundamentally different macro-  
429 catchments show changes in WBC predominantly during the wet season, with strongest  
430 effects for the conversion of native vegetation (Cerrado and rainforest) to pasture.
- 431 • In the das Mortes catchment with the more pronounced dry season, the ground water  
432 components are more relevant for annual discharge generation. The more seasonal  
433 climate also coincides with more pronounced LUC effects on hydrology at the beginning  
434 of the rainy season, whereas under less seasonal rainforest climate ( $\leq 3$  arid month), LUC  
435 effects on hydrology are apparent during the whole rainy season.

436 Acknowledgements:

437 This study was carried out in the framework of the integrated project CarBioCial funded by the  
438 German Ministry of Education and Research (BMBF) under the grant number 01LL0902F.

439 References:

- 440 Abbaspour KC. 2007. User manual for SWAT-CUP, SWAT calibration and uncertainty analysis  
441 programs. *Swiss Federal Institute of Aquatic Science and Technology, Eawag, Duebendorf,*  
442 *Switzerland.*
- 443 Abbaspour KC, Johnson CA, van Genuchten MT. 2004. Estimating uncertain flow and transport  
444 parameters using a sequential uncertainty fitting procedure. *Vadose Zone Journal* **3**(4): 1340. DOI:  
445 10.2136/vzj2004.1340.
- 446 Allen RG, Pereira LS, Raes D, Smith M, others. 1998. Crop evapotranspiration-Guidelines for  
447 computing crop water requirements-FAO Irrigation and drainage paper 56. *FAO, Rome* **300**(9).
- 448 Amoozegar A, Warrick AW. 1986. Hydraulic Conductivity of Saturated Soils: Field Methods. *Methods*  
449 *of Soil Analysis: Part 1—Physical and Mineralogical Methods* 735–770. DOI:  
450 10.2136/sssabookser5.1.2ed.c29.
- 451 Arima EY, Richards P, Walker R, Caldas MM. 2011. Statistical confirmation of indirect land use change  
452 in the Brazilian Amazon. *Environmental Research Letters* **6**(2): 24010. DOI: 10.1088/1748-  
453 9326/6/2/024010.
- 454 Arnold JG, Moriasi DN, Gassman PW, Abbaspour KC, White MJ, Srinivasan R, Santhi C, Harmel RD,  
455 Van Griensven A, Van Liew MW, others. 2012. SWAT: Model use, calibration, and validation.  
456 *Transactions of the ASABE* **55**(4): 1491–1508.
- 457 Barona E, Ramankutty N, Hyman G, Coomes OT. 2010. The role of pasture and soybean in  
458 deforestation of the Brazilian Amazon. *Environmental Research Letters* **5**(2): 24002.
- 459 Beuchle R, Grecchi RC, Shimabukuro YE, Seliger R, Eva HD, Sano E, Achard F. 2015. Land cover  
460 changes in the Brazilian Cerrado and Caatinga biomes from 1990 to 2010 based on a systematic  
461 remote sensing sampling approach. *Applied Geography* **58**: 116–127. DOI:  
462 10.1016/j.apgeog.2015.01.017.
- 463 Beven K. 2010. *Environmental modelling: an uncertain future?* CRC Press: Routledge.
- 464 Böhner J. this issue. Paradigm in modelling climate change – results with STAR and WRF. .
- 465 Böhner J, Dietrich H, Fraedrich K, Kawohl T, Kilian M, Lucarini V, Lunkeit F. 2013. Development and  
466 implementation of a hierarchical model chain for modelling regional climate variability and climate  
467 change over southern Amazonia. *Interdisciplinary Analysis and Modeling of Carbon-Optimized Land*  
468 *Management Strategies for Southern Amazonia, Universitätsdrucke Göttingen* 119–128.
- 469 Bozana Maciocheck. 2013. Change Detection im Wassereinzugsgebiet Novo Progresso (Pará,  
470 Brasilien). Göttingen, Germany.
- 471 Bronstert A, Niehoff D, Bürger G. 2002. Effects of climate and land-use change on storm runoff  
472 generation: present knowledge and modelling capabilities. *Hydrological Processes* **16**(2): 509–529.  
473 DOI: 10.1002/hyp.326.
- 474 Bruijnzeel LA. 2004. Hydrological functions of tropical forests: not seeing the soil for the trees?  
475 *Agriculture, Ecosystems & Environment* **104**(1): 185–228. DOI: 10.1016/j.agee.2004.01.015.

- 476 Chiang L, Chaubey I, Gitau MW, Arnold JG. 2010. Differentiating impacts of land use changes from  
477 pasture management in a CEAP watershed using the SWAT model. *Trans. ASABE* **53**(5): 1569–1584.
- 478 Christoffersen BO, Restrepo-Coupe N, Arain MA, Baker IT, Cestaro BP, Ciais P, Fisher JB, Galbraith D,  
479 Guan X, Gulden L, others. 2014. Mechanisms of water supply and vegetation demand govern the  
480 seasonality and magnitude of evapotranspiration in Amazonia and Cerrado. *Agricultural and Forest  
481 meteorology* **191**: 33–50. DOI: 10.1016/j.agrformet.2014.02.008.
- 482 Cleveland WS. 1981. LOWESS: A program for smoothing scatterplots by robust locally weighted  
483 regression. *American Statistician* 54–54. DOI: 10.2307/2683591.
- 484 Climate-Data.org. 2015. *Climate data for cities worldwide*. <http://en.climate-data.org/>, Accessed 27  
485 May 2015.
- 486 Coe MT, Costa MH, Soares-Filho BS. 2009. The influence of historical and potential future  
487 deforestation on the stream flow of the Amazon River – Land surface processes and atmospheric  
488 feedbacks. *Journal of Hydrology* **369**(1–2): 165–174. DOI: 10.1016/j.jhydrol.2009.02.043.
- 489 Costa MH, Botta A, Cardille JA. 2003. Effects of large-scale changes in land cover on the discharge of  
490 the Tocantins River, Southeastern Amazonia. *Journal of Hydrology* **283**(1–4): 206–217. DOI:  
491 10.1016/S0022-1694(03)00267-1.
- 492 D’Almeida C, Vörösmarty CJ, Hurtt GC, Marengo JA, Dingman SL, Keim BD. 2007. The effects of  
493 deforestation on the hydrological cycle in Amazonia: a review on scale and resolution. *International  
494 Journal of Climatology* **27**(5): 633–647. DOI: 10.1002/joc.1475.
- 495 Davidson EA, de Araújo AC, Artaxo P, Balch JK, Brown IF, C. Bustamante MM, Coe MT, DeFries RS,  
496 Keller M, Longo M, Munger JW, Schroeder W, Soares-Filho BS, Souza CM, Wofsy SC. 2012. The  
497 Amazon basin in transition. *Nature* **481**(7381): 321–328. DOI: 10.1038/nature10717.
- 498 De Paiva RCD, Buarque DC, Collischonn W, Bonnet M-P, Frappart F, Calmant S, Bulhões Mendes CA.  
499 2013. Large-scale hydrologic and hydrodynamic modeling of the Amazon River basin. *Water  
500 Resources Research* **49**(3): 1226–1243. DOI: 10.1002/wrcr.20067.
- 501 De Roo A, Odijk M, Schmuck G, Koster E, Lucieer A. 2001. Assessing the effects of land use changes  
502 on floods in the Meuse and Oder catchment. *Physics and Chemistry of the Earth, Part B: Hydrology,  
503 Oceans and Atmosphere* **26**(7): 593–599.
- 504 DeFries R, Eshleman KN. 2004. Land-use change and hydrologic processes: a major focus for the  
505 future. *Hydrological Processes* **18**(11): 2183–2186. DOI: 10.1002/hyp.5584.
- 506 Drewry JJ, Cameron KC, Buchan GD. 2008. Pasture yield and soil physical property responses to soil  
507 compaction from treading and grazing — a review. *Soil Research* **46**(3): 237–256. DOI:  
508 10.1071/SR07125.
- 509 ESALQ. 2015. *Escola Superior de Agricultura “Luiz de Queiroz.”* <http://www.esalq.usp.br/gerd/>  
510 Accessed 1 June 2015.
- 511 Fearnside PM. 2005. Deforestation in Brazilian Amazonia: history, rates, and consequences.  
512 *Conservation biology* **19**(3): 680–688. DOI: 10.1111/j.1523-1739.2005.00697.x.
- 513 Fearnside PM. 2007. Brazil’s Cuiabá-Santarém (BR-163) Highway: the environmental cost of paving a  
514 soybean corridor through the Amazon. *Environmental management* **39**(5): 601–614.

515 Fuka DR, Walter MT, MacAlister C, Degaetano AT, Steenhuis TS, Easton ZM. 2014. Using the Climate  
516 Forecast System Reanalysis as weather input data for watershed models. *Hydrological Processes*  
517 **28**(22): 5613–5623. DOI: 10.1002/hyp.10073.

518 Fukunaga DC, Cecílio RA, Zanetti SS, Oliveira LT, Caiado MAC. 2015. Application of the SWAT  
519 hydrologic model to a tropical watershed at Brazil. *CATENA* **125**: 206–213. DOI:  
520 10.1016/j.catena.2014.10.032.

521 Galford GL, Melillo J, Mustard JF, Cerri CEP, Cerri CC. 2010. The Amazon Frontier of Land-Use Change:  
522 Croplands and Consequences for Greenhouse Gas Emissions. *Earth Interactions* **14**(15): 1–24. DOI:  
523 10.1175/2010EI327.1.

524 Gassman PW, Reyes MR, Green CH, Arnold JG. 2007. Soil and Water Assessment Tool: Historical  
525 Development, Applications, and Future Research Directions, The. *Center for Agricultural and Rural*  
526 *Development Iowa State University Working Paper 07-WP 443*.

527 George C. 2014. Simulation of Hydrologic Impacts of Land Use Land Cover Changes in a Humid  
528 Tropical River Basin. .

529 Giambelluca TW, Scholz FG, Bucci SJ, Meinzer FC, Goldstein G, Hoffmann WA, Franco AC, Buchert  
530 MP. 2009. Evapotranspiration and energy balance of Brazilian savannas with contrasting tree density.  
531 *Agricultural and Forest Meteorology* **149**(8): 1365–1376. DOI: 10.1016/j.agrformet.2009.03.006.

532 Global Weather Data. 2015. <http://globalweather.tamu.edu/> Accessed 31 May 2015.

533 Göpel J, Schaldach R. this issue. Sustainable land management in Southern Amazonia: Model-based  
534 analysis of the robustness of carbon-optimized management systems under global change pressures.  
535 .

536 Granier A, Loustau D, Bréda N. 2000. A generic model of forest canopy conductance dependent on  
537 climate, soil water availability and leaf area index. *Annals of Forest Science* **57**(8): 11. DOI:  
538 10.1051/forest:2000158.

539 Guse B, Pfannerstill M, Fohrer N. 2015. Dynamic modelling of land use change impacts on nitrate  
540 loads in rivers. *Environmental Processes* **2**(4): 575–592.

541 Guzha A, Nobrega R, Kovacs K, Amorim RSS, Gerold G. 2013a. Quantifying impacts of agro-industrial  
542 expansion in Mato Grosso, Brazil, on watershed hydrology using the Soil and Water Assessment Tool  
543 (SWAT) model. paper presented at the Conference: 20th International Congress on Modelling and  
544 Simulation. Adelaide, Australia. DOI: 10.5194/hessd-12-9915-2015.

545 Guzha A, Nobrega R, Santos C, Gerold G. 2013b. Investigating discharge and rainfall variability in an  
546 Amazonian watershed: Do any trends exist? *IAHS-AISH publication* 346–351.

547 Hayhoe SJ, Neill C, Porder S, Mchorney R, Lefebvre P, Coe MT, Elsenbeer H, Krusche AV. 2011.  
548 Conversion to soy on the Amazonian agricultural frontier increases streamflow without affecting  
549 stormflow dynamics. *Global Change Biology* **17**(5): 1821–1833. DOI: 10.1111/j.1365-  
550 2486.2011.02392.x.

551 Hodnett MG, da Silva LP, da Rocha HR, Cruz Senna R. 1995. Seasonal soil water storage changes  
552 beneath central Amazonian rainforest and pasture. *Journal of Hydrology* **170**(1–4): 233–254. DOI:  
553 10.1016/0022-1694(94)02672-X.

- 554 Hunke P, Mueller EN, Schröder B, Zeilhofer P. 2015a. The Brazilian Cerrado: assessment of water and  
555 soil degradation in catchments under intensive agricultural use. *Ecohydrology* **8**(6): 1154–1180. DOI:  
556 10.1002/eco.1573.
- 557 Hunke P, Roller R, Zeilhofer P, Schröder B, Mueller EN. 2015b. Soil changes under different land-uses  
558 in the Cerrado of Mato Grosso, Brazil. *Geoderma Regional* **4**: 31–43. DOI:  
559 10.1016/j.geodrs.2014.12.001.
- 560 Jacomine PKT. 2013. A nova classificacao brasileira de solos. *Anais da Academia Pernambucana de*  
561 *Ciência Agronômica* **5**(0): 161–179.
- 562 Kergoat L. 1998. A model for hydrological equilibrium of leaf area index on a global scale. *Journal of*  
563 *Hydrology* **212–213**: 268–286. DOI: 10.1016/S0022-1694(98)00211-X.
- 564 Koch FJ, van Griensven A, Uhlenbrook S, Tekleab S, Teferi E. 2012. The Effects of Land use Change on  
565 Hydrological Responses in the Choke Mountain Range (Ethiopia)-A new Approach Addressing Land  
566 Use Dynamics in the Model SWAT. *Proceedings of 2012 International Congress on Environmental*  
567 *Modeling and Software Managing Resources of a Limited Planet, Sixth Biennial Meeting, Leipzig,*  
568 *Germany, 1–5.*
- 569 Lambin EF, Turner BL, Geist HJ, Agbola SB, Angelsen A, Bruce JW, Coomes OT, Dirzo R, Fischer G,  
570 Folke C, George PS, Homewood K, Imbernon J, Leemans R, Li X, Moran EF, Mortimore M,  
571 Ramakrishnan PS, Richards JF, Skånes H, Steffen W, Stone GD, Svedin U, Veldkamp TA, Vogel C, Xu J.  
572 2001. The causes of land-use and land-cover change: moving beyond the myths. *Global*  
573 *Environmental Change* **11**(4): 261–269. DOI: 10.1016/S0959-3780(01)00007-3.
- 574 Lathuillière MJ, Johnson MS, Donner SD. 2012. Water use by terrestrial ecosystems: temporal  
575 variability in rainforest and agricultural contributions to evapotranspiration in Mato Grosso, Brazil.  
576 *Environmental Research Letters* **7**(2): 24024. DOI: 10.1088/1748-9326/7/2/024024.
- 577 Lima LS, Coe MT, Filho BSS, Cuadra SV, Dias LCP, Costa MH, Lima LS, Rodrigues HO. 2013. Feedbacks  
578 between deforestation, climate, and hydrology in the Southwestern Amazon: implications for the  
579 provision of ecosystem services. *Landscape Ecology* **29**(2): 261–274. DOI: 10.1007/s10980-013-9962-  
580 1.
- 581 Lima W de P, Zakia MB, Libardi PL, de Souza Filho AP, others. 1990. Comparative evapotranspiration  
582 of eucalyptus, pine and natural “cerrado” vegetation measure by the soil water balance method”.  
583 *Ipef International, Piracicaba.*
- 584 Macedo MN, DeFries RS, Morton DC, Stickler CM, Galford GL, Shimabukuro YE. 2012. Decoupling of  
585 deforestation and soy production in the southern Amazon during the late 2000s. *Proceedings of the*  
586 *National Academy of Sciences* **109**(4): 1341–1346. DOI: 10.1073/pnas.1111374109.
- 587 Macioscheck B. 2013. Land use classification upper Jamanxim catchment. ESRI ArcGIS shape files.  
588 Göttingen, Germany.
- 589 Maia SMF, Ogle SM, Cerri CEP, Cerri CC. 2010. Soil organic carbon stock change due to land use  
590 activity along the agricultural frontier of the southwestern Amazon, Brazil, between 1970 and 2002.  
591 *Global Change Biology* **16**(10): 2775–2788. DOI: 10.1111/j.1365-2486.2009.02105.x.
- 592 Mani A, Devi MU, Ramulu V, others. 2014. Simulation of Impact of Change in Landuse on Water Yield  
593 of Upper Manair Catchment. *International Journal of Innovative Research and Development* **3**(1).

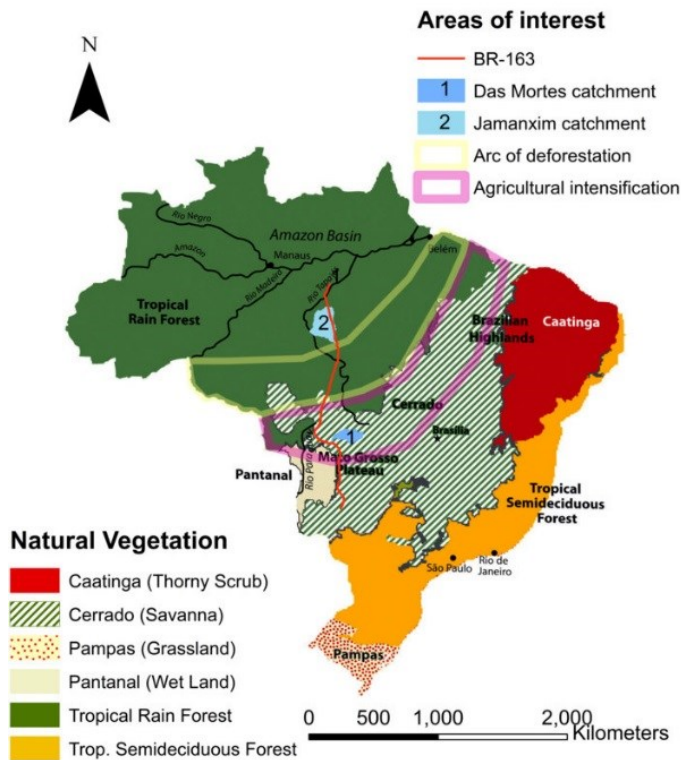


- 594 McGrath DA, Smith CK, Gholz HL, Oliveira F de A. 2001. Effects of Land-Use Change on Soil Nutrient  
595 Dynamics in Amazônia. *Ecosystems* **4**(7): 625–645. DOI: 10.1007/s10021-001-0033-0.
- 596 Miles L, Newton AC, DeFries RS, Ravilious C, May I, Blyth S, Kapos V, Gordon JE. 2006. A global  
597 overview of the conservation status of tropical dry forests. *Journal of Biogeography* **33**(3): 491–505.  
598 DOI: 10.1111/j.1365-2699.2005.01424.x.
- 599 Mishra SK, Singh VP. 2003. *Soil Conservation Service Curve Number (SCS-CN) Methodology*. Springer  
600 Science & Business Media.
- 601 Moriasi DN, Arnold JG, Van Liew MW, Bingner RL, Harmel RD, Veith TL. 2007. Model evaluation  
602 guidelines for systematic quantification of accuracy in watershed simulations. *Trans. ASABE* **50**(3):  
603 885–900.
- 604 Müller H, Rufin P, Griffiths P, Barros Siqueira AJ, Hostert P. 2015. Mining dense Landsat time series  
605 for separating cropland and pasture in a heterogeneous Brazilian savanna landscape. *Remote Sensing  
606 of Environment* **156**: 490–499. DOI: 10.1016/j.rse.2014.10.014.
- 607 Nandakumar N, Mein RG. 1997. Uncertainty in rainfall—runoff model simulations and the  
608 implications for predicting the hydrologic effects of land-use change. *Journal of Hydrology* **192**(1–4):  
609 211–232. DOI: 10.1016/S0022-1694(96)03106-X.
- 610 Negri AJ, Adler RF, Xu L, Surratt J. 2004. The impact of Amazonian deforestation on dry season  
611 rainfall. *Journal of Climate* **17**(6): 1306–1319.
- 612 Nobre CA, Sellers PJ, Shukla J. 1991. Amazonian Deforestation and Regional Climate Change. *Journal  
613 of Climate* **4**(10): 957–988. DOI: 10.1175/1520-0442(1991)004<0957:ADARCC>2.0.CO;2.
- 614 Nobrega RLB, A. C. Guzha, G. N. Torres, K. Kovacs, G. Lamparter, R. S. S. Amorim, E. Couto, G. Gerold.  
615 2015. Identifying hydrological responses of micro-catchments under contrasting land use in the  
616 Brazilian Cerrado. *Hydrology and Earth System Sciences* **19**. DOI: 10.5194/hessd-12-9915-2015.
- 617 Oliveira PS. 2014. Balanço hídrico e erosão do solo no Cerrado Brasileiro. Sao Paulo, School of  
618 engineering, department of hydraulics and sanitary engineering.
- 619 Oliveira PTS, Nearing MA, Moran MS, Goodrich DC, Wendland E, Gupta HV. 2014. Trends in water  
620 balance components across the Brazilian Cerrado. *Water Resources Research* **50**(9): 7100–7114. DOI:  
621 10.1002/2013WR015202.
- 622 Pai N, Saraswat D. 2011. SWAT 2009 \_LUC: A Tool to Activate the Land Use Change Module in SWAT  
623 2009. *Transactions of the ASABE* **54**(5): 1649–1658.
- 624 Pongratz J, Bounoua L, DeFries RS, Morton DC, Anderson LO, Mauser W, Klink CA. 2006. The Impact  
625 of Land Cover Change on Surface Energy and Water Balance in Mato Grosso, Brazil. *Earth Interactions*  
626 **10**(19): 1–17. DOI: 10.1175/EI176.1.
- 627 Price K. 2011. Effects of watershed topography, soils, land use, and climate on baseflow hydrology in  
628 humid regions: A review. *Progress in physical geography* **35**(4): 465–492.
- 629 Rodrigues ASL, Ewers RM, Parry L, Souza C, Veríssimo A, Balmford A. 2009. Boom-and-Bust  
630 Development Patterns Across the Amazon Deforestation Frontier. *Science* **324**(5933): 1435–1437.  
631 DOI: 10.1126/science.1174002.

- 632 Schaldach R, Alcamo J, Koch J, Kölking C, Lapola DM, Schüngel J, Priess JA. 2011. An integrated  
633 approach to modelling land-use change on continental and global scales. *Environmental Modelling &*  
634 *Software* **26**(8): 1041–1051. DOI: 10.1016/j.envsoft.2011.02.013.
- 635 Schaldach R, Koch J. 2009. Conceptual design and implementation of a model for the integrated  
636 simulation of large-scale land-use systems. In: Athanasiadis DIN, Rizzoli PAE, Mitkas PA and Gómez  
637 PD-IJM (eds) *Information Technologies in Environmental Engineering*. Springer Berlin Heidelberg,  
638 425–438, DOI:10.1007/978-3-540-88351-7\_32.
- 639 Scheffler R, Neill C, Krusche AV, Elsenbeer H. 2011. Soil hydraulic response to land-use change  
640 associated with the recent soybean expansion at the Amazon agricultural frontier. *Agriculture,*  
641 *Ecosystems & Environment* **144**(1): 281–289. DOI: 10.1016/j.agee.2011.08.016.
- 642 Schilling KE, Jha MK, Zhang Y-K, Gassman PW, Wolter CF. 2008. Impact of land use and land cover  
643 change on the water balance of a large agricultural watershed: Historical effects and future  
644 directions. *Water Resources Research* **44**(7): W00A09. DOI: 10.1029/2007WR006644.
- 645 Schlicht S. 2013. Dynamics of deforestation and agricultural production in the upper Rio das Mortes  
646 watershed in Mato Grosso state (Brazil). M.Sc thesis, Göttingen, Germany, University of Göttingen.
- 647 Schneider R. 1963. *Groundwater Proviceces Brazil*. Prepared in coopertaion with the Government of  
648 Brazil and the United Staes Operation Mission to Brazil. Washington, USA.
- 649 Schönenberg R, Hartberger, Korbinian, Schumann, Charlotte, Guggenberger, Georg, Siebold, Mathias,  
650 Boy, Jens, Lakes, Lamparter, Gabriele, Schindewolf, Marcus, Nendel, Claas, Hohnwald, Stefan, Gerold,  
651 Gerhard, Klingler, Michael. this issue. Methods of inter- and transdisciplinary research – a trajectory  
652 of knowledge integration. .
- 653 Sellers PJ, Randall D a., Collatz G j., Berry J a., Field C b., Dazlich D a., Zhang C, Collelo G d., Bounoua L.  
654 1996. A Revised Land Surface Parameterization (SiB2) for Atmospheric GCMS. Part I: Model  
655 Formulation. *Journal of Climate* **9**(4): 676–705. DOI: 10.1175/1520-  
656 0442(1996)009<0676:ARLSPF>2.0.CO;2.
- 657 Sellers PJ, Shuttleworth WJ, Dorman JL, Dalcher A, Roberts JM. 1989. Calibrating the Simple  
658 Biosphere Model for Amazonian Tropical Forest Using Field and Remote Sensing Data. Part I: Average  
659 Calibration with Field Data. *Journal of Applied Meteorology* **28**(8): 727–759. DOI: 10.1175/1520-  
660 0450(1989)028<0727:CTSBMF>2.0.CO;2.
- 661 Strauch M, Volk M. 2013. SWAT plant growth modification for improved modeling of perennial  
662 vegetation in the tropics. *Ecological Modelling* **269**: 98–112. DOI: 10.1016/j.ecolmodel.2013.08.013.
- 663 usouthal.edu. 2016. *Brzilian Geological Map*. .
- 664 Wagner PD, Bhallamudi SM, Narasimhan B, Kantakumar LN, Sudheer KP, Kumar S, Schneider K,  
665 Fiener P. 2016. Dynamic integration of land use changes in a hydrologic assessment of a rapidly  
666 developing Indian catchment. *Science of The Total Environment* **539**: 153–164. DOI:  
667 10.1016/j.scitotenv.2015.08.148.
- 668 Wertz-Kanounnikoff SA. 2005. Forest policy enforcement at the Amazon frontier : the case of Mato  
669 Grosso, Brazil. Dissertation.
- 670 ZEE ZEE. 2015. , <http://www.zee.mg.gov.br/>. <http://www.zee.mg.gov.br/> Accessed 31 May 2015.

671

672



673

674 *Figure :1 Vegetation biomes in Brazil, locations of the study catchments, the BR-163 and the current*  
 675 *extent of the Amazon agricultural frontier (base map from “Forests in Brazil” 2015; frontier*  
 676 *reproduced after “Global Forest Watch” 2015)*

677 *Table 1: Main land use types during the historic calibration and validation period (Landsat imagery*  
 678 *evaluation and \*statistical data) and for future LUC scenarios (developed with LANDSHIFT (Göpel and*  
 679 *Schaldach, this issue)*

	Das Mortes catchment			Jamanxim catchment		
<b>Historic</b>	<b>1970</b>	<b>1988</b>	<b>1998</b>	<b>1998</b>	<b>2007</b>	<b>2011</b>
Cerrado and Forest	97.5*	64.26	39.79	95.34	91.42	85.03
Cropland	-	-	-	0.10	0.03	0.09
Non-Forest/Pasture	2.00*	35.57	59.89	4.34	8.34	14.57
<b>Trend Scenario</b>	<b>2020</b>	<b>2025</b>	<b>2030</b>	<b>2020</b>	<b>2025</b>	<b>2030</b>
Cerrado and Forest	12.53	11.42	10.96	83.31	79.59	77.20
Cropland	54.31	54.31	54.31	9.91	10.06	10.09
Pasture	32.93	34.04	34.50	5.42	9.17	11.61
<b>Sustainable Scenario</b>	<b>2020</b>	<b>2025</b>	<b>2030</b>	<b>2020</b>	<b>2025</b>	<b>2030</b>
Cerrado and Forest	13.24	12.42	11.66	88.10	88.10	88.10
Cropland	64.29	65.70	67.12	9.90	9.90	10.04
Pasture	22.25	21.65	21.00	0.21	0.21	0.08
<b>Legal Int. Scenario</b>	<b>2020</b>	<b>2025</b>	<b>2030</b>	<b>2020</b>	<b>2025</b>	<b>2030</b>
Cerrado and Forest	14.00	13.61	13.40	82.30	76.67	65.24
Cropland	63.92	64.31	64.48	7.46	12.29	23.71
Pasture	21.86	21.86	21.89	10.04	10.04	10.04
<b>Illegal Int. Scenario</b>	<b>2020</b>	<b>2025</b>	<b>2030</b>	<b>2020</b>	<b>2025</b>	<b>2030</b>
Cerrado and Forest	17.05	16.66	16.39	69.94	66.82	64.56
Cropland	60.58	60.97	61.23	18.14	21.20	23.46
Pasture	22.15	22.14	22.16	11.04	11.14	11.17

680 Table 2: Optimum calibration parameter values for land use dependent top soil parameters

Land use	Das Mortes				Jamanxim		
	Gallery forest	Non-Forest Pasture	Non-Forest Cropland	Cerrado		Rain-forest	Pasture
CN	44	58	48	35		36	60
$k_{sat}$ Latosolo vermelho mm h <sup>-1</sup>	183		117	262	$k_{sat}$ Argilosolo mm h <sup>-1</sup>	461	453
$k_{sat}$ Latosolo Vermelho amarelo mm h <sup>-1</sup>	559		407	594	$k_{sat}$ Latosolo vermelho-amarelo mm h <sup>-1</sup>	670	587
$k_{sat}$ Neosolo mm h <sup>-1</sup>	103	120		224	$k_{sat}$ Neosolo mm h <sup>-1</sup>	221	212

681

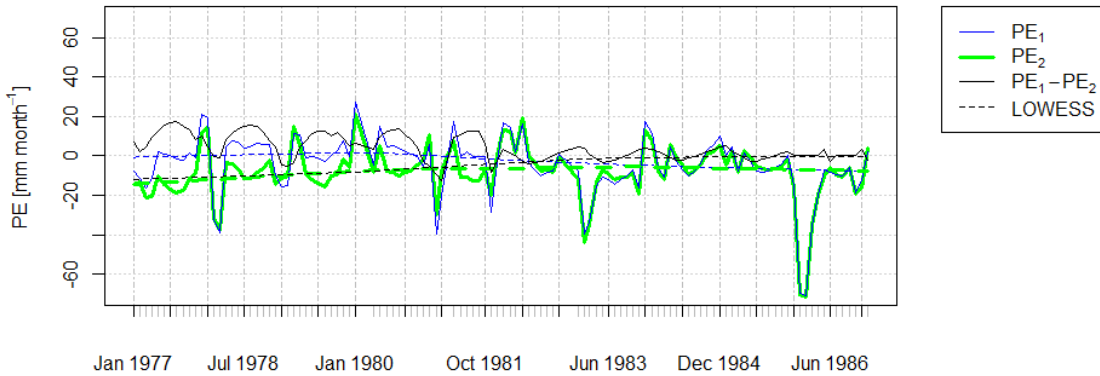
682 Table 3: Calibration Statistics for the Model calibration, validation and steady land use application in both study catchments  
 683 for a monthly time step calibration (coefficient of determination: R<sup>2</sup>, Nash-Sutcliffe Efficiency index: NS, percentual bias:  
 684 PBIAS, p- and r-factor of the 95% confidence interval)

	Das Mortes					Jamanxim				
	R <sup>2</sup>	NS	PBIAS	p-factor	r-factor	R <sup>2</sup>	NS	PBIAS	p-factor	r-factor
Calibration	0.85	0.74	-4.54	0.84	0.87	0.8	0.8	-0.5	0.60	0.47
Validation	0.79	0.73	-8.1	0.91	0.86	0.8	0.8	0.8	0.42	0.63
steady land use	0.84	0.61	-16.4	0.81	0.99	0.8	0.8	1.7	0.52	0.48

685

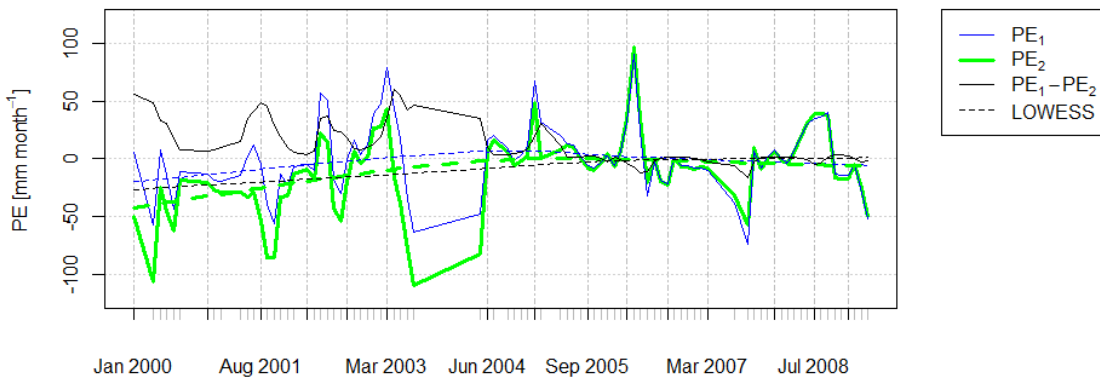
686

Prediction errors das Mortes catchment



687

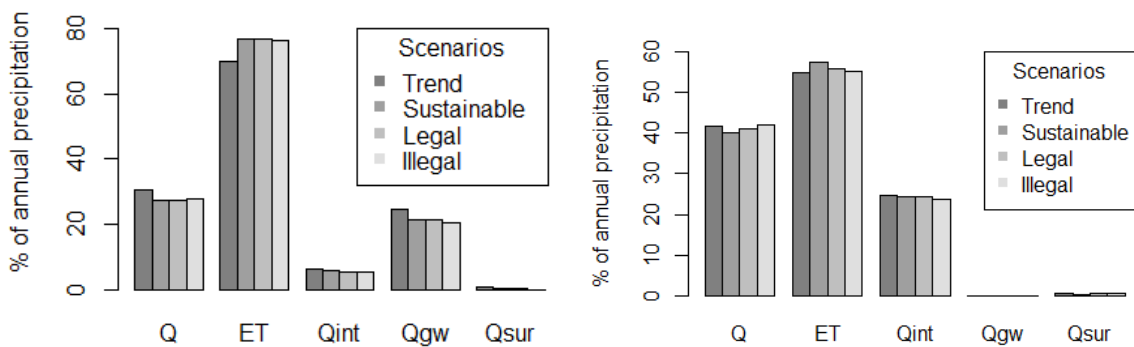
Prediction errors Jamanxim catchment



688

689 *Figure 2a Das Mortes catchment model, Prediction Error*  
 690 *(PE=Qobs-Qmod) of the land use update (PE₁) and steady*  
 691 *land use (PE₂) setup, difference in PE (PE₁-PE₂) and LOWESS*  
 692 *trend lines of all latter, for the calibration and validation*

693 *2b Jamanxim catchment model, Prediction Error (PE=Qobs-*  
 694 *Qmod) of the land use update (PE₁) and steady land use (PE₂)*  
 695 *setup, difference in PE (PE₁-PE₂) and LOWESS trend lines of all*  
 696 *latter, for the calibration and validation*



697

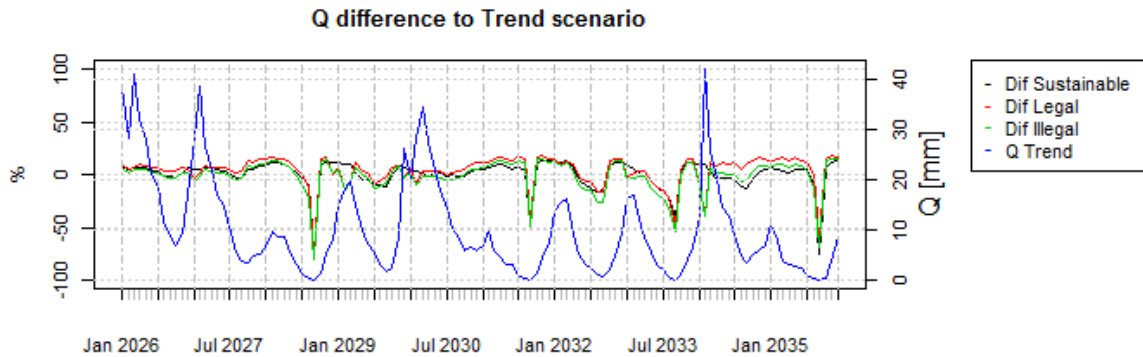
698

699 *Figure 3 a and b*

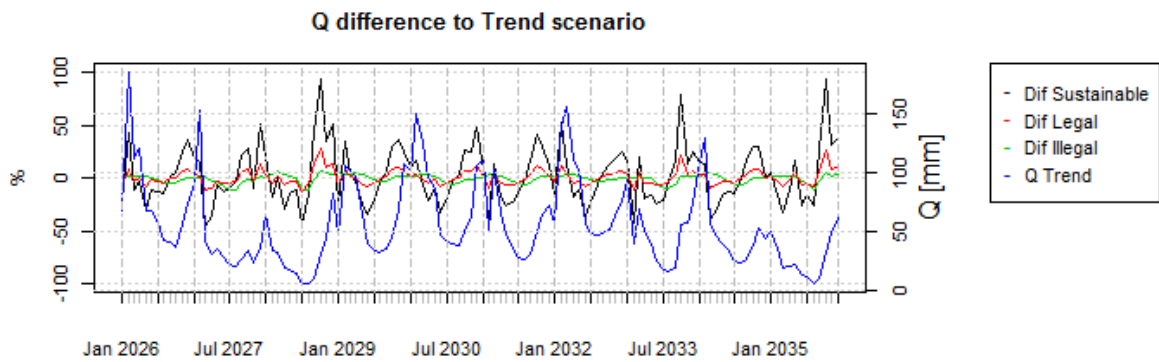
700 *Das Mortes catchment; annual water balance components in relation to mean annual rainfall for model scenario period*  
 701 *2026 to 2035, Q: discharge, ET: Evapotranspiration, Qint: interflow from shallow aquifer, Qgw: Groundwater or Baseflow*  
 702 *contribution to discharge, Qsur: Surface runoff contribution to discharge*

703 *Jamanxim catchment, annual water balance components in relation to mean annual rainfall for model scenario period 2026*  
 704 *to 2035, Q: discharge, ET: Evapotranspiration, Qint: interflow from shallow aquifer, Qgw: Groundwater or Baseflow*  
 705 *contribution to discharge, Qsur: Surface runoff contribution to discharge*

706



707



708 *Figure 4 a: Difference in scenario predicted stream discharge:  $\Delta Q = Q_{trend} - Q_{other\ scenarios}$ , and*  
 709 *simulated stream discharge for trend scenario, das Mortes catchment*  
 710

711 *Figure 5 b: Difference in scenario predicted stream discharge:  $\Delta Q = Q_{trend} - Q_{other\ scenarios}$ , and*  
 712 *simulated stream discharge for trend scenario, Jamanxim catchment*

713

714

715

716